Frequency response of multipactor discharge

Agust Valfells, R. A. Kishek, and Y. Y. Lau
Department of Nuclear Engineering and Radiological Sciences, University of Michigan, Ann Arbor, Michigan 48109-2104

(Received 13 May 1997; accepted 22 September 1997)

This paper analyzes the frequency response of a two-surface multipactor in a rf circuit. An equation for the frequency band in which steady state multipactor can occur is derived in terms of the secondary emission properties of the surface, the quality factor Q of the rf circuit, and the operating voltage. The steady-state multipactor current is also derived, and is shown to be in excellent agreement with numerical computations that follow the temporal evolution of the multipactor discharge. © *1998 American Institute of Physics.* [S1070-664X(98)00501-1]

I. INTRODUCTION

Multipactor discharge is a medium- to low-voltage phenomenon frequently observed in microwave systems.[1–5] Its presence often requires little more than an ac electric field on a metallic surface[1,6–9] or on a dielectric surface[2,10] under a moderately high vacuum condition.[11] While known for more than 60 years,[9] multipactor received only spotty theoretical treatments until recently, when a concerted effort has been made to understand its evolution,[6,7] its conditions for existence,[6–12] its saturation mechanism,[6,8] its saturation level,[8] and its dependence on the properties of the materials and on the electrical properties of the rf circuit.[8,9] With few exceptions, most of these studies were concentrated on two-surface multipactor, such as that which would occur across the gap of a rf cavity.

In assessing the interaction between the multipactor with a rf circuit, it has been assumed[7–9] that the external rf source, which initiates the multipactor discharge, is at a frequency that is the same as the cold-tube natural frequency of the rf circuit. Under such an assumption, it was found that multipactor saturates by its loading of the rf circuit as the multipactor current grows. This finding is restricted, because of space charge effects, to quality factor Q of the rf structure greater than about 10, and to maximum secondary yield less than about 1.5, so that the multipactor growth is not rapid. If a steady state is indeed reached, multipactor may consume tens of percent of the external rf power,[8] with the impact energy of the secondary electrons equal to the first cross-over point in the secondary electron yield curve (i.e., E_1 in Fig. 2 below).

In this paper, we extend our previous work to analyze the frequency response of multipactor discharge in a rf circuit. Specifically, we assume that the external rf source's frequency does not necessarily coincide with the cold tube frequency of the rf circuit. In this way, we may gain a deeper understanding of multipactor discharge under more general conditions. The use of a highly simplied model allows us to derive the frequency band over which steady-state multipactor may exist, as well as the saturation level of the multipactor current under these more general conditions. We restrict our study to first-order two-surface multipactor.[1] We ignore the effects of external magnetic field and of a random emission velocity distribution of the secondary electrons.

II. THE MODEL

The model is shown in Fig. 1. The rf structure is represented by a circuit [with resistance R, inductance L, capacitance C, quality factor Q, and characteristic frequency $\omega_0 = (LC)^{-1/2}$] connected to parallel plates, between which a single electron sheet of charge density, σ, oscillates. This electron sheet represents the multipactor electrons. The gap voltage is provided by an ideal current source $I_d = I_{d0}\sin(\omega t+\phi)$. The gap spacing is D. The frequency response may be examined by varying ω about ω_0.

Normalized parameters are used in the analysis. The normalizing factors are: D for distance; ω_0 for frequency; $1/\omega_0$ for time; $v=\omega_0 D$ for velocity; $U=mv^2$ for energy; $V=U/e$ for voltage (e is the magnitude of the electron charge); $E=V/D$ for electric field; $\Sigma=\varepsilon_0 E$ for the surface charge density (ε_0 is the free space permittivity); and V/Z for current, where $Z=(L/C)^{1/2}$ is the intrinsic impedance of the circuit. The governing (normalized) equations are (Fig. 1)

$$\left(\frac{d^2}{dt^2}+\frac{1}{Q}\cdot\frac{d}{dt}+1\right)V(t)=\frac{d}{dt}\left(I_{d0}\sin(\omega\cdot t+\phi)+I_m(t)\right), \tag{1}$$

$$I_m(t)=-\sigma\cdot\frac{d}{dt}x(t), \tag{2}$$

$$\frac{d^2}{dt^2}x(t)=V(t)+\sigma\cdot\left(x-\frac{1}{2}\right), \tag{3}$$

where V is the gap voltage, I_m is the multipactor current, and x is the normalized position in the gap. Equation (1) is the circuit equation for the gap voltage V, Eq. (2) gives the multipactor current induced as a result of the motion of the charge sheet, and Eq. (3) is the force law which describes the action on the electron sheet by the gap voltage V and by the image charge. Note that *although the image charge term in (3), the last term of (3), is included in the computer simulations, the steady-state theory ignores it.* This may be justified because in the $Q>10$ cavities studied in this paper, beam loading saturates the charge density to such a low level that the space charge force term in (3) is negligible. This is also evident in Fig. 8 below, where the simulation results (that include the space charge force) agree well with the analytic

 1070-664X/98/5(1)/300/5/$15.00

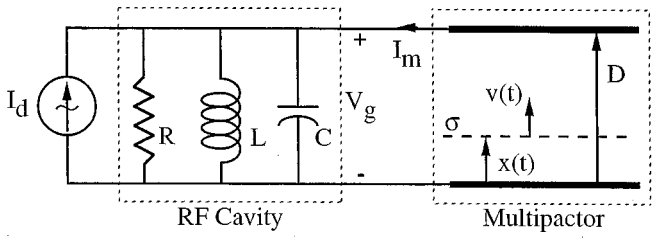

FIG. 1. Model of multipactor discharge in the parallel plate cavity.

theory (that does not include the space charge force). It is also important to note that, in the evaluation of the stability boundary (e.g., Figs. 3 and 5–7), we may ignore the space charge force altogether, because on the stability boundary there can be no growth of multipactor charge from an infinitesimal value. Also note that, in general, the space charge density, σ, is constant, except at impact when it may experience a step-like change because of secondary emission.[13]

A modified version of Vaughan's formula for the secondary electron emission coefficient is used:[14]

$$\delta=\delta_{\max}\cdot(w\ \exp(1-w))^k, \tag{4}$$

where $w=E_i/E_{\max}$, E_i is the impact energy of the incident electron, $E_{\max}$ is the energy at which the maximun value $\delta_{\max}$ occurs (Fig. 2), and $k=0.62$ for $w<1$, and $k=0.25$ for $w>1$. The energies, for which $\delta=1$, are E_1 and E_2; E_1 being the lower value is the ''first cross over energy.''

III. STEADY-STATE THEORY AND COMPARISON WITH NUMERICAL RESULTS

Equations (1)–(4) describe the temporal evolution of the multipactor discharge in a rf circuit whose normalized cold tube natural frequency is unity, and whose unloaded quality factor is Q. To evaluate the frequency response of the multipactor, we assume that the external rf current source I_{d0} will have a variable frequency ω in the neighborhood of unity. Regardless of ω, when steady state is reached, the space charge density σ is constant. The impact energy equals the energy at the first crossover point, E_1, of the yield curve in Fig. 2 (corresponding to an impact velocity of μ), and the gap must be crossed in half a rf period. Thus, upon ignoring the image charge term in Eq. (3), we integrate Eq. (3) twice to obtain

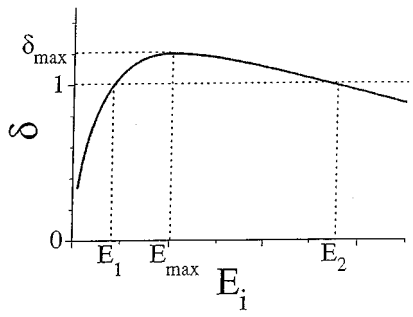

FIG. 2. Typical secondary electron yield curve.

$$\int_0^{\pi/\omega}V(t)\ dt=\mu-u_0, \tag{5}$$

$$\int_0^{\pi/\omega}\left(\int_0^{\tau}V(t)\ dt\right)\ d\tau=1-\frac{\pi}{\omega}\cdot u_0, \tag{6}$$

where u_0 is the emission velocity of the secondary electrons (assumed to be uniform).

Let $V_0(t)$ denote the gap voltage going from $x(t=0)=0$ to $x(t=\pi/\omega)=1$, and $V_1(t)$ denote the gap voltage going from $x(t=0)=1$ to $x(t=\pi/\omega)=0$. Solving (1)–(3), with the steady-state condition, $V_0(t)=-V_1(t)$, and using the jump condition on $V(t)$ at impact, we obtain

$$V_0(t)=\exp\left(\frac{-t}{2Q}\right)(A\ \cos(\omega_1\cdot t)+B\ \sin(\omega_1\cdot t))$$
$$+C\ \cos(\omega\cdot t-\zeta), \tag{7}$$

where

$$A=\left(\frac{\sigma\cdot\eta\cdot(\mu-u_0)\sin\ \psi}{\omega_1\cdot(1+\eta^2+2\,\eta\ \cos\ \psi)}\right), \tag{8}$$

$$B=-\left(\frac{\sigma\cdot(\mu-u_0)(1+\eta\ \cos\ \psi}{\omega_1\cdot(1+\eta^2+2\,\eta\ \cos\ \psi)}\right), \tag{9}$$

$$C=\frac{I_{d0}\omega}{\sqrt{(1+\sigma-\omega^2)^2+\dfrac{\omega^2}{Q^2}}}, \tag{10}$$

$$\omega_1^2=1+\sigma-\frac{1}{4Q^2}, \tag{11}$$

$$\eta=\exp\left(-\frac{\pi}{2Q\omega}\right), \tag{12}$$

$$\psi=\pi\cdot\frac{\omega_1}{\omega}. \tag{13}$$

One uses conditions (5) and (6) to determine any two of the parameters ζ (the impact phase), σ, or ω, given the value of the third.

Figure 3 shows the region in which steady-state multipactor occurs for a typical case. Steady state is only obtained when the initial sheet is launched within the bounded area. The abscissa is the phase angle of the driver current when the initial electron sheet is emitted. The ordinate is the normalized frequency of the rf voltage. The diagonal parts of the boundary are due to rapid quenching of the multipactor discharge (in very few rf cycles), as the secondary electrons are emitted at an unfavorable phase of the gap voltage. The horizontal parts of the boundary are due to the fact that the amplitude of the gap voltage is not great enough to accelerate electrons to an impact velocity μ. This latter boundary sets the outer limits of the frequency which can sustain a multipactor discharge.

Simulations show that the steady-state charge density of the multipactor discharge goes smoothly from a maximum value near $\omega=1$, to zero at the frequency boundary. *Since the*

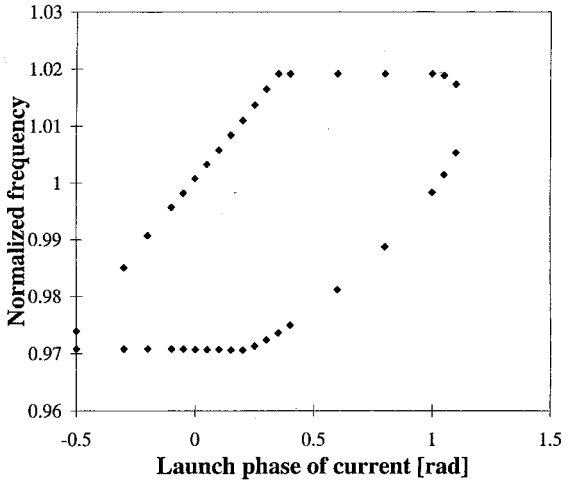

FIG. 3. Stability band of multipactor discharge, from simulation: $Q=10$, $\mu=0.491$, and normalized operating voltage=0.3.

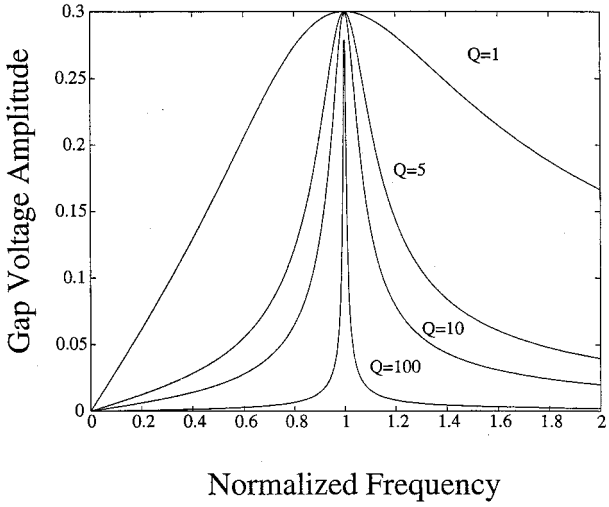

FIG. 4. Response curves of gap voltage for an unloaded cavity. Fixed operating voltage of 0.3, differing Q-values.

transient terms in the solution for the gap voltage are directly proportional to the charge density, they can be ignored at the frequency limits, hence

$$V(t)=C\,\cos(\omega\cdot t-\zeta). \tag{14}$$

Imposing conditions (5) and (6) on (14) yields the following equations for the impact phase of the gap voltage, and frequency limits, respectively:

$$\zeta=\text{atan}\left(\frac{2(\mu-u_0)}{2\omega-\pi\cdot(\mu+u_0)}\right), \tag{15}$$

$$\omega^2=1-\frac{1}{2Q^2}\pm\sqrt{\frac{(2I_{d0}\,\sin\,\zeta)^2}{(\mu-u_0)^2}-\frac{1}{Q^2}+\frac{1}{4Q^4}}, \tag{16}$$

which has solutions $\omega_{\max}$ and $\omega_{\min}$. Note that the right-hand side of (16) is only weakly dependent upon ω through ζ, and thus Eq. (16) may be either solved graphically, or approximately by using the value of ζ ($\omega=1$) in Eq. (15). Using this approximation one may take the width of the stability band to be

$$W\equiv\omega_{\max}-\omega_{\min}$$
$$\approx\frac{2}{(\omega_{\max}+\omega_{\min})Q}\sqrt{\frac{(2QI_{d0}\,\sin\,\zeta)^2}{(\mu-u_0)^2}-1+\frac{1}{4Q^2}}, \tag{17}$$

where $\zeta=\zeta\,(\omega=1)$.

Note from Eq. (16) that for large values of Q the frequency limits are nearly symmetric about $\omega=1$. If one defines the operating voltage as the amplitude of the gap voltage when $\omega=1$ and $\sigma=0$ (operating voltage$=I_{d0}Q$), then *for a fixed operating voltage and large value of Q one finds* $W\sim 1/Q$. It is also clear that for a fixed (large) Q, then W is nearly proportional to the operating voltage. The reason for this is straightforward: To accelerate the electrons across the gap, so as to reach the impact velocity, μ, a minimum amplitude of the gap voltage is needed. The response for a fixed operating voltage is narrowed with higher Q, thus narrowing the frequency band. Increasing the operating voltage raises the response curves, thus widening the frequency band. Figure 4 shows how the amplitude of the gap voltage varies with frequency, in an unloaded cavity, with a fixed operating voltage. Figure 5 shows how the frequency band is dependent upon the Q value for a fixed operating voltage, comparing the results of Eq. (16) to those of computer simulation. Figure 6 shows how the frequency band varies with operating voltage for a fixed value of Q, once again comparing the results of Eq. (16) to those of computer simulation. The effects of varying the surface material and/or emission velocity are not as straightforward, since ζ is a strong function of μ and u_0. Figure 7 shows the effects of the emission velocity on the frequency band as calculated from Eq. (16). It should be stressed that the above analysis yields a necessary condition for steady-state multipactor to be obtainable. Other mechanisms can deny access to the steady state.

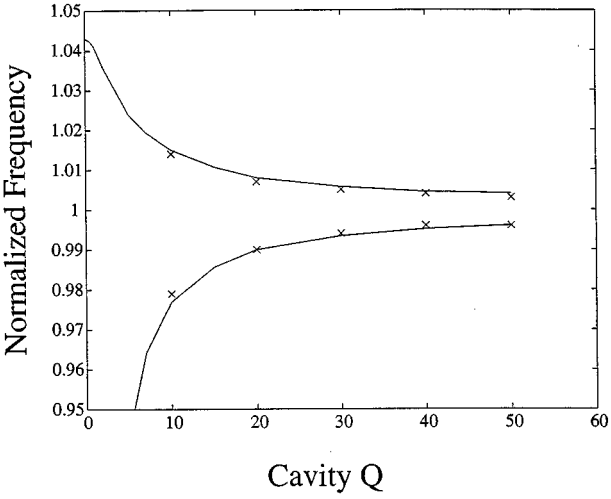

FIG. 5. Stability band as a function of cavity Q. Operating voltage=0.3, $\mu=0.543$. Solid line is from Eq. (16), x symbols are from simulation.

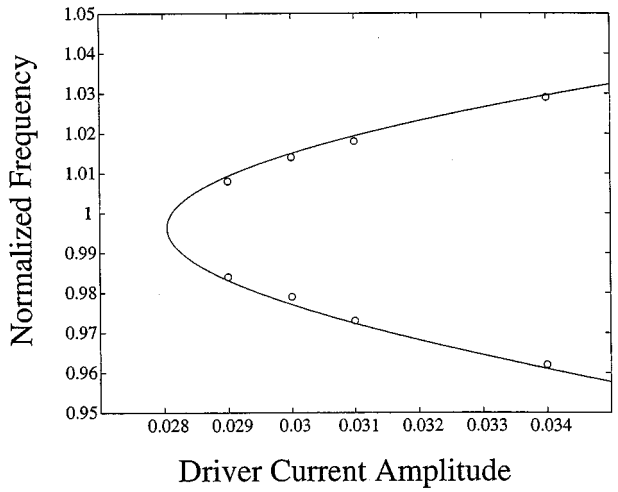

FIG. 6. Stability band as a function of operating voltage. $Q=10$, $\mu=0.543$. Solid line is from Eq. (16); o symbols are from simulation

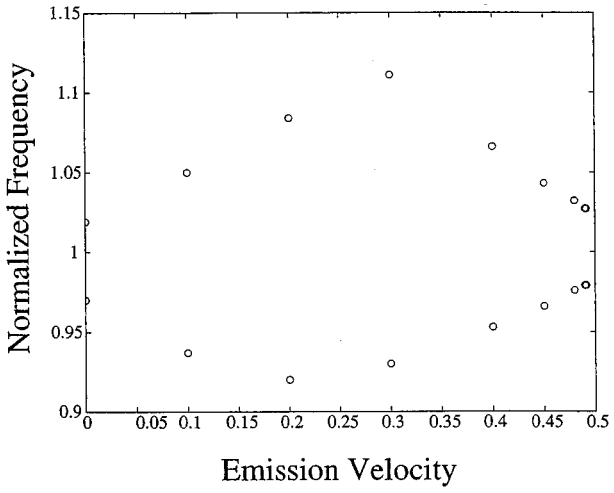

FIG. 7. Stability band as function of emission velocity as calculated from Eq. 16. $Q=10$, operating voltage$=0.3$.

It is of interest to calculate the steady-state charge density of the multipactor. This can be done by using the full equation for $V(t)$ and imposing conditions (5) and (6), then getting a graphical solution. A quicker method is to approximate the phase angle by use of Eq. (15), and then using only the condition given by Eq. (5). The resulting implicit equation for the steady-state charge is

$$\mu-u_0=\frac{[A(1-\eta\cdot\cos\psi)-B\eta\sin\psi]/2Q+(B(1-\eta\cdot\cos\psi)+A\eta\cdot\sin\psi)\omega_1}{1+\sigma}+\left(\frac{2C\sin\zeta}{\omega}\right), \tag{18}$$

which is easily solved graphically. Results of Eq. (18) are compared to computer simulations in Fig. 8.

IV. CONCLUDING REMARKS

The analysis presented above is by no means exhaustive, but it does yield necessary—if not sufficient—conditions for the existence of steady-state, first-order multipactor in planar geometry. It is found that the stability band is roughly symmetric about the natural frequency of the rf circuit. The width of the stability band is found to be inversely proportional to the Q of the cavity, for a fixed operating voltage, while it is found to increase linearly with operating voltage, for a fixed value of Q. Effects of emission velocity and secondary emission characteristics are given implicitly in Eq. (16). Finally an approximate, implicit, equation for the steady-state charge density of the discharge is presented. Since our simulations include the combined effects of off-resonant driving, of the beam loading by the multipactor, and of the image charge, what is given here is a reasonably complete study of the frequency response of the multipactor discharge, for $Q>10$ and $\delta_{\max}<1.5$.

Finally, we should remark that space charge forces are indeed important for very low Q structures (i.e., nonresonant structures), in which the rf field is less responsive to whatever multipactor growth. They may also be important even in a high Q cavity, if the secondary yield substantially exceeds unity. In the latter case, saturation may be due to both cavity detuning and space charge forces which give rise to charge debunching and field reversal.[15] The relative importance between the two saturation mechanisms remains to be examined.

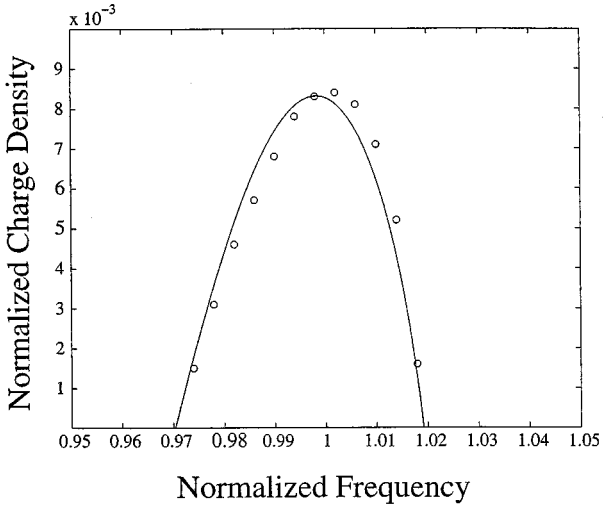

FIG. 8. Steady-state charge density of multipactor. Operating voltage$=0.3$, $Q=10$, $\mu=0.491$. Solid line is from Eq. (18), open circles are from simulation.

ACKNOWLEDGMENTS

This work was supported by the Department of Navy Grant No. N00014-97-1-G001 issued by the Naval Research Laboratory, and by the Multidisciplinary University Research Initiative (MURI), managed by the Air Force Office of Scientific Research and subcontracted through Texas Tech University.

[1]J. R. M. Vaughan, IEEE Trans. Electron Devices **ED-15**, 883 (1968); **ED-35**, 1172 (1988).
[2]D. H. Preist and R. C. Talcott, IEEE Trans. Electron Devices **ED-8**, 243 (1961).
[3]J. R. M. Vaughan, IEEE Trans. Electron Devices **ED-8**, 302 (1961).
[4]S. Yamaguchi, Y. Saito, S. Anami, and S. Michizono, IEEE Trans. Nucl. Sci. **39**, 278 (1992).
[5]P. F. Clancy, Microw. J. **21**, 77 (March 1978); N. Rozario, H. F. Lenjing, K. F. Reardon, M. S. Zarro, and C. G. Baran, IEEE Trans. Microwave Theory Tech. **MTT-42**, 558 (1994); A. D. Woode and J. Petit, Microw. J. **35**, 142 (January 1992); R. Woo, Proc. Inst. Electr. Eng. **57**, 254 (1969).
[6]S. Riyopoulos, D. Chernin, and D. Dialetis, Phys. Plasmas **2**, 3194 (1995); IEEE Trans. Electron Devices **ED-44**, 489 (1997); S. Riyopolous, Phys. Plasmas **4**, 1448 (1997).
[7]R. Kishek and Y. Y. Lau, Phys. Rev. Lett. **75**, 1218 (1995); Phys. Plasmas **3**, 1481 (1996).
[8]R. A. Kishek, Y. Y. Lau, and D. Chernin, Phys. Plasmas **4**, 863 (1997).
[9]R. A. Kishek, Ph.D. Thesis, University of Michigan, Ann Arbor, (1997).
[10]R. A. Kishek and Y. Y. Lau, ''Multipactor discharge on a dielectric,'' to appear in Phys. Rev. Lett.
[11]F. Hohn, W. Jacob, R. Beckmann, and R. Wilhelm, Phys. Plasmas **4**, 940 (1997).
[12]V. P. Gopinath, private communications (1996).
[13]O. Hachenberg and W. Brauer, Adv. Electron. Electron Phys. **XI**, 413 (1959); C. K. Birdsall and W. B. Bridges, *Electron Dynamics of Diode Regions* (Academic, New York, 1966).
[14]J. R. M. Vaughan, IEEE Trans. Electron Devices **ED-36**, 1963 (1989); A. Shih and C. Hor, IEEE Trans. Electron Devices **ED-40**, 824 (1993).
[15]S. Riyopolous, Phys. Plasmas **4**, 1448 (1997).